Ultrasensitive Detection of Mitochondrial DNA Mutation by Graphene Oxide/DNA Hydrogel Electrode

*Liping Sun, Nan Hu, Jian Peng, Liyu Chen, and Jian Weng**

Ultrasensitive detection of nucleic acid has attracted considerable attention recently in academic research and clinic diagnostics. Current approaches for DNA analysis involve complicated or expensive processes for labeling and often yield a high detection limit. In this study, a hydrogel electrode prepared from graphene oxide and fish sperm DNA is used for label–free mitochondrial DNA detection by impedimetric approach. The hydrogel has a bionic structure containing rich water and natural biomolecule fish sperm DNA that would benefit the adsorption and hybridization of DNA. Graphene oxide is a semiconductor and its conductivity can be improved by doping negatively charged DNA molecules. The result shows that the conductivity and impedance change of hydrogel electrode could be tuned by its length and component. The linear range for DNA detection by the optimized hydrogel is from 1.0×10^{-9} to 1.0×10^{-20} M with a detection limit of 1.0×10^{-20} M. The result is ascribed to the bionic structure and tunable conductivity of hydrogel electrode. The hydrogel electrode has been used to detect the real DNA samples from patients of ovarian cancer with satisfactory results.

1. Introduction

The extremely low detection limit of DNA biosensor is essential for its applications in medical diagnostics and genetic screening.[1] The label–free detection of DNA by electrochemical method, without use of any specialized reagent, would greatly simplify the analysis technique and accelerate its implementation for rapid DNA sequencing and diagnostics.[2] The design of electrode with a bionic structure containing rich water and biomolecules and tunable conductivity would play an important role in improving the sensitivity of electrochemical detection of DNA. The bionic structure benefits the adsorption and hybridization of DNA.[3] The intermediate conductivity of electrode is sensitive to the change of conductivity introduced by trace DNA on the surface of electrode. On the contrary, this weak change is unobvious for the electrode with too high or low conductivity. As is well known, the conductivity of semiconductor silicon can be increased by adding certain impurities in minute quantities. Graphene oxide (GO) is a semiconductor and its conductivity can be improved by doping negatively charged molecules.[4] Therefore, the conductivity of hydrogel containing GO, water and natural biomolecules would be very sensitive to negatively charged molecules, such as DNA, and this hydrogel could be developed as novel DNA biosensor with high sensitivity.

Fish sperm DNA is a natural DNA extracted from fish sperm and could form hydrogel with GO.[5] The GO/DNA hydrogel contains three components: GO, fish sperm DNA and water. Every component plays an important role in improving the sensitivity of DNA detection. GO is a semiconductor with intermediate conductivity compared with its reduced form (RGO) and most polymers,[6] which might produce a large conductivity change when trace DNA molecule was introduced. The hydrogel contains a large amount of fish sperm DNA molecules that could provide much higher biocompatibility than that of other chemical cross–linkers, which is advantageous for DNA hybridization in this bionic structure. The hydrogel also contains rich water that is similar to the natural environment for DNA hybridization, which is also beneficial to improving the hybridization efficiency of DNA. In addition, the hydrogel has a large specific surface and high diffusivity of small molecules[7] besides the biocompatibility. Therefore, it is a viable candidate for sensory and actuation applications. The sensitivity of biosensor is influenced by the conductivity of hydrogel which depends upon its thickness and component.[8] Conventionally, the hydrogel is simply coated onto the surface of classical electrodes, which makes the shape and thickness of hydrogel irregular and uncontrollable, respectively. One possible route is to form the hydrogel directly in a tube so that the shape would be fixed and the thickness could be controlled as needed. The conductivity of hydrogel could be tuned by changing its component and thickness.

Herein, we reported a hydrogel electrode prepared from GO and fish sperm DNA (**Scheme 1**). The mixed solution of GO and

Dr. L. P. Sun,[+] N. Hu,[+] J. Peng, Prof. J. Weng
Department of Biomaterials
College of Materials
Xiamen University
Xiamen, 361005, P.R. China
E-mail: jweng@xmu.edu.cn
L. Y. Chen
Zhongshan Hospital
Xiamen University
Xiamen, 361004, P.R. China
Prof. J. Weng
ShenZhen Research Institute of Xiamen University
Shenzhen, 518057, P.R. China
[+]L.P.S. and N.H. contributed equally to this work.

DOI: 10.1002/adfm.201402191

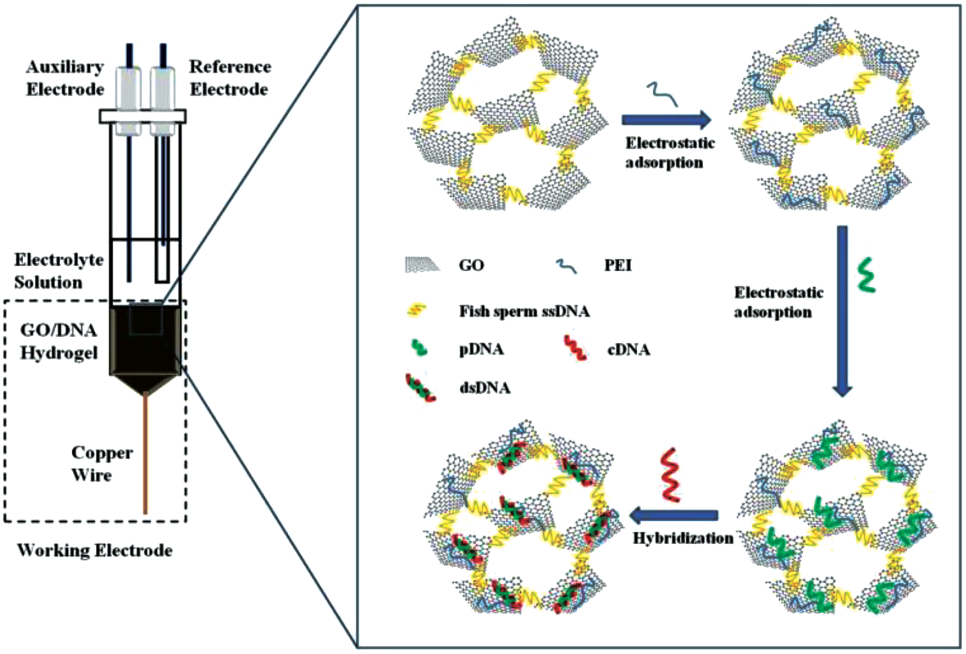

Scheme 1. Schematic of DNA detection by GO/DNA hydrogel electrode. (left) Schematic of the experimental set-up employed for the impedance measurement of DNA. (right) Schematic immobilization of pDNA and hybridization with cDNA on GO/DNA hydrogel electrode. GO: graphene oxide; PEI: polyethylenimine; ssDNA: single-stranded DNA; pDNA: probe DNA; cDNA: complementary DNA; dsDNA: double-stranded DNA.

fish sperm DNA in a cone bottom-centrifuge tube was heated to produce GO/DNA hydrogel. A copper wire was inserted into the cone bottom of centrifuge tube to form GO/DNA hydrogel electrode as the working electrode (Scheme S1, Supporting Information). This hydrogel electrode was successfully used to detect mitochondrial DNA mutation with high sensitivity and selectivity. The detection principle is that the impedance will obviously decrease after hybridization of complementary DNA (cDNA) with probe DNA (pDNA) immobilized on the GO/DNA hydrogel electrode, which is due to the higher conductivity of GO doped by double-stranded DNA (dsDNA) than that of single-stranded DNA (ssDNA). The change of impedance is unobvious after pDNA hybrids with mismatched or non–complementary DNAs, which is due to the low hybridization efficiency. Therefore, mismatched sequences can be distinguished from perfectly matched cDNA by measuring the change of impedance. The hydrogel electrode has also been used to detect the real DNA samples from patients of ovarian cancer with satisfactory results.

2. Results and Discussion

2.1. Electrochemical Properties of Hydrogel Electrode

GO was synthesized from graphite by the modified Hummers method as carried out in our previous work.[9] The GO/DNA hydrogel in a centrifuge tube was prepared by simply heating the mixed solution of GO and fish sperm DNA at 95 °C for 5 min[5] and characterized well (Figure S1–3, Supporting Information). Then GO/DNA hydrogel was used as working electrode (Scheme 1). The negatively charged GO/DNA hydrogel is difficult to adsorb the negatively charged pDNA due to electrostatic repulsion. Therefore, cationic polymer polyethylenimine (PEI) was first adsorbed to the GO/DNA electrode by electrostatic attraction, which resulted in the impedance increasing (**Figure 1**a). This indicates that the electrode was very sensitive to the adsorbate, which is of advantage to improve the sensitivity of electrode. At the same time, the impedance of GO/DNA hydrogel electrode increased with the hydrogel volume (or thickness) increasing (Figure 1b and Table S1 in Supporting Information). Therefore, the conductivity of GO/DNA hydrogel electrode can be tuned by its volume (or thickness) to produce an optimal conductivity for improving the sensitivity of electrode in the following DNA detection.

To build a simple model, the hydrogel electrode/electrolyte interface based on Randles equivalent circuit is divided into two physical regions: the bulk electrolyte solution, the electrode layer (including hydrogel, PEI and binding DNA). The respective components correspond to (1) R_s, the ohmic resistance of the electrolyte solution; and (2) R, a parallel combination of the charge–transfer resistance R_{ct}, Warburg impedance Z_w and capacitance C_d. Thus, R can also be quite sensitive to the adsorption of pDNA and following hybridization with cDNA.

pDNA (Table S2, Supporting Information) was adsorbed on PEI–modified GO/DNA hydrogel electrode (PEI–hydrogel) by electrostatic attraction to produce pDNA/PEI–hydrogel electrode. We have investigated the effect of pDNA concentration and hydrogel volume on the immobilization time of pDNA. The optimal immobilization time and pDNA concentration were about 30 min and 100 nM (Figure S4, Supporting Information), respectively. 100 nM pDNA concentration and 30 min of immobilization time were used in following measurements. The high pDNA concentration and long immobilization time were advantageous to adsorb more pDNA molecules and blocked free

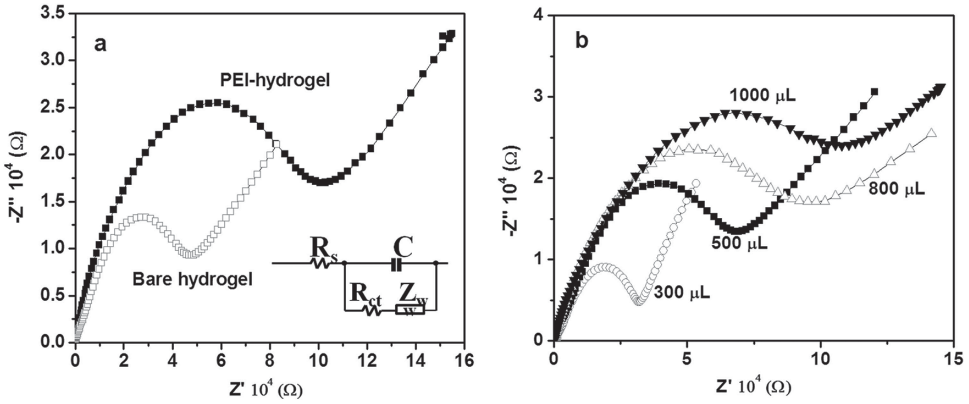

Figure 1. a) Impedance of GO/DNA hydrogel electrode before and after modification with PEI. Inset: equivalent circuit used to model impedance data in the presence of redox couples. Rs, electrolyte solution resistance; R_{ct}, element of interfacial electron transfer resistance; C, capacitance of the electric double layer between electrolyte and interface of electrode. b) Impedance of GO/DNA hydrogel with different volumes. Nyqiust curves were attained in 5.0 mM $[Fe(CN)_6]^{3-/4-}$ and 1.0 M KCl solution.

amino groups of PEI, which will guarantee that all cDNA would hybrid with pDNA in the following hybridization step instead of the adsorption though electrostatic attraction. A large drop in impedance was measured when cDNA was added into pDNA/PEI–hydrogel electrode (**Figure 2**). This result is due to the higher conductivity of GO doped by dsDNA and less secondary structure of dsDNA with respect to ssDNA,[10] which is supported by the cyclic voltammetry data (Figure S5, Supporting Information). The largest impedance change was obtained at 0.5 mL of GO/DNA hydrogel (Figure 2 and Table S3 in Supporting Information). The result means that the hydrogel with too high or low conductivity was not sensitive to the change of conductivity introduced by DNA on the surface of electrode. The intermediate conductivity of electrode is very important to the sensitivity of hydrogel for DNA detector. Therefore, 0.5 mL of GO/DNA hydrogel electrode was used in the following measurements. The hybridization efficiency also depends strictly on hybridization temperature. **Figure 3** shows that resistance changes (ΔR) would increase with decreasing temperature. The result is reasonable because the melting temperature of DNA is about 57 °C and the dsDNA would separate into ssDNA when the temperature is close to its melting temperature. Therefore, the optimal hybridization temperature is 25 °C.

2.2. Detection of DNA Mutation

We designed 4 pairs of different pDNA and cDNA sequences (Table S2, Supporting Information). 4 PEI–hydrogel electrodes were prepared and each electrode was immobilized with one of the pDNA and hybridized with its respective cDNA, respectively. The impedances of all electrodes experienced obvious decrease after incubation with corresponding cDNA, and similar resistance changes (ΔR) could be observed (Figure S6, Supporting Information), indicating high universality of this hydrogel electrode for DNA detection. P1 and C1 were used in the following measurements unless specially mentioned. The impedance of pDNA/PEI–hydrogel electrode decreased with increasing concentration of cDNA (**Figure 4**a). The resistance change ΔR after hybridization is linear with the logarithm of cDNA concentrations (Figure 4b) from 1.0×10^{-20} to 1.0×10^{-9} M (ΔR = 0.41logC + 10.7, correlation coefficient of 0.99). The increase of resistance change ΔR for concentration higher than 10^{-9} M is unobvious, indicating that the sensor became saturated. The detection limit of 1.0×10^{-20} M (the signal-to-noise ratio is 2) was lower than that of other graphene electrodes (Table S4, Supporting Information).[11] We also checked the background signal of GO/DNA hydrogel. The impedance

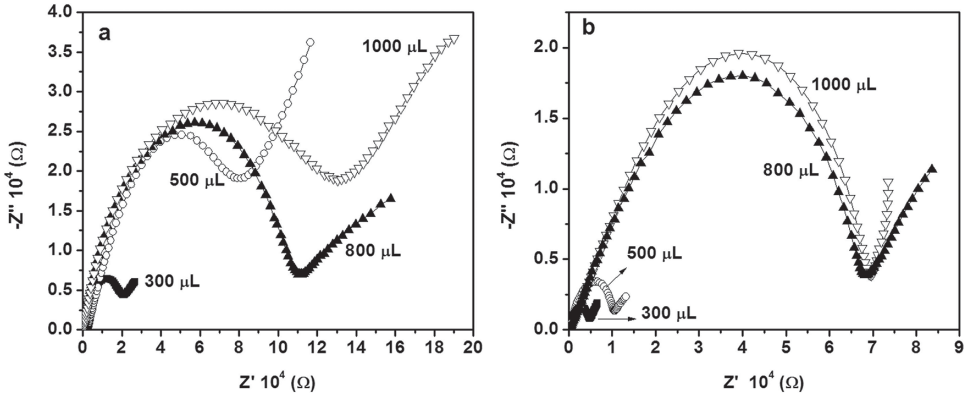

Figure 2. Impedance of pDNA/PEI–hydrogel with different volumes before (a) and after (b) hybridization with cDNA. The concentrations of pDNA and cDNA were 100 nM and 1.0×10^{-9} M, respectively.

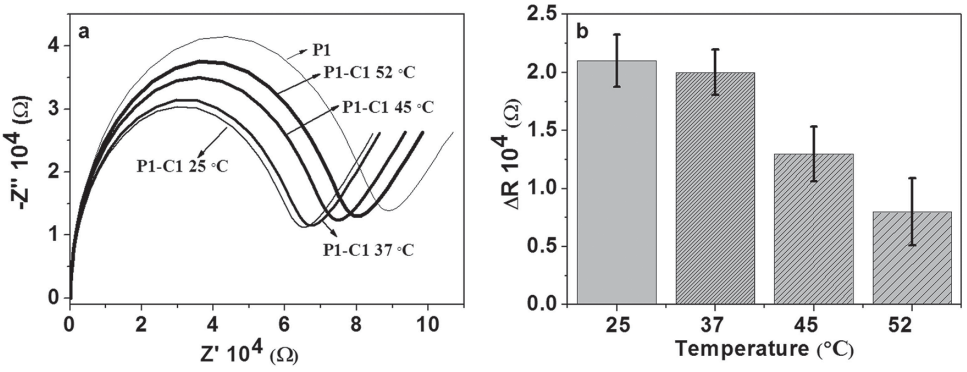

Figure 3. a) Nyquist diagrams of pDNA/PEI–hydrogel electrode before (P1) and after (P1-C1) hybridization with cDNA at 25, 37, 45 and 52 °C. b) ΔR of pDNA/PEI–hydrogel electrode after hybridization with cDNA at 25, 37, 45 and 52 °C. The concentrations of pDNA and cDNA were 100 nM and 1.0×10^{-18} M, respectively.

values of pDNA/PEI-Hydrogel in cDNA solution (1.0×10^{-20} M) and blank solution are obviously distinguishing (Figure S7, Supporting Information). The result indicates that the GO/DNA hydrogel electrode could be used to detect DNA without labelling by electrochemical impedance with a high sensitivity.

To explore the selectivity of pDNA/PEI–hydrogel electrode, target DNAs with varying number of mutations were designed (Table S5, Supporting Information). ΔR values decreased in the following orders: cDNA > one–base mismatch > two–base mismatch > three–base mismatch > non–complementary DNAs (Figure 4c). Therefore, the identification of cDNA, mismatched or non–complementary DNAs can be referred to the resistance change ΔR. Usually, it is easier to differentiate cDNA from muitiple-base mismatched DNA than from single-base mismatched DNA. However, in our hydrogel electrode system, single–base mismatched DNA showed 80% signal reduction compared with cDNA, indicating high selectivity of this electrode for detection of single-base mismatch. The 80% signal reduction for one–base mismatch is lower than that of other electrodes.[12] The high sensitivity and selectivity of hydrogel

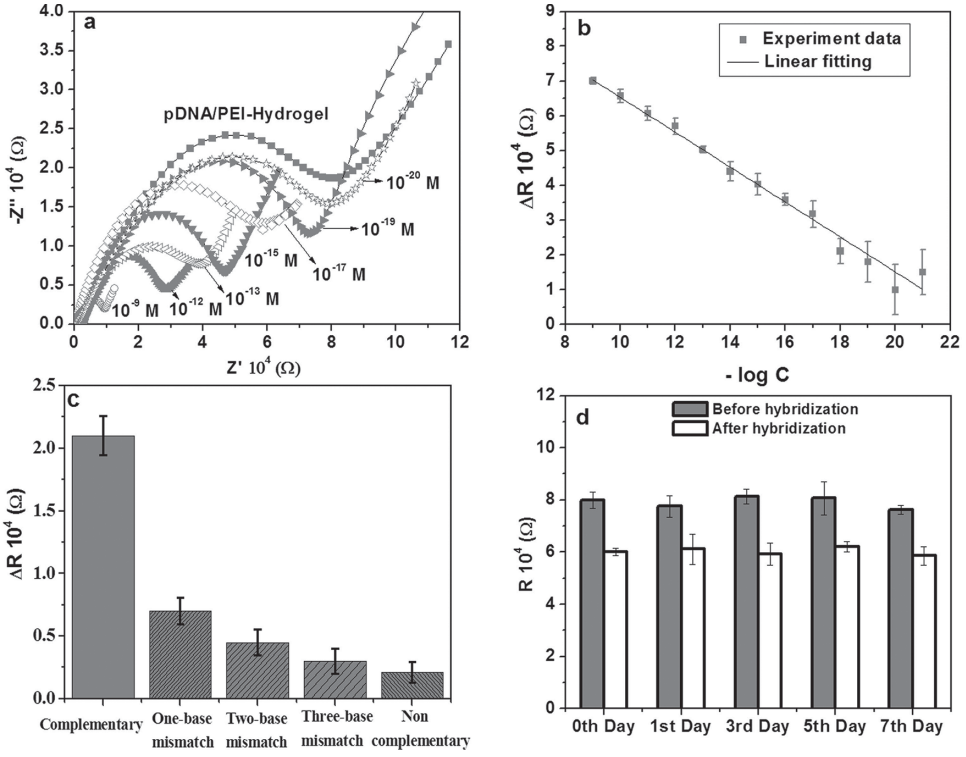

Figure 4. Detection of mitochondrial DNA mutation 16223 C–T by electrochemical impedance. a) Nyquist diagrams of pDNA/PEI–hydrogel electrode before and after hybridization with cDNA with different concentrations. b) Calibration plot of ΔR for detecting cDNA. c) ΔR of pDNA/PEI–hydrogel electrode after hybridization with 1.0×10^{-18} M cDNA, 1.0×10^{-9} M one–base mismatched, two–base mismatched, three–base mismatched and non–complementary DNAs. (d) The stability of pDNA/PEI–hydrogel electrode. Data are the mean ± standard deviation of three different experiments. pDNA and target DNA sequences are listed in Table S5 (Supporting Information).

electrode might be attributed to the bionic structure and tunable conductivity of hydrogel electrode. Moreover, the impedances before and after hybridization were changed little even when the electrode was stored in refrigerator (4 °C) for 7 days (Figure 4d). Therefore, the hydrogel electrode has a very high selectivity and stability. In addition, we also investigated the detection limit of this electrode for other two mitochondrial DNA mutations: 709G-A and 489T-C (Figure S8 and Table S6, Supporting Information). The similar detection limits were obtained, indicating universality of this hydrogel electrode for DNA detection.

2.3. Confirmation of DNA Hybridization in Hydrogel

In order to confirm DNA hybridization in hydrogel, Hoechst 33258, a DNA minor groove binder and electrochemically active dye,[13] was added into hydrogel electrode before and after hybridization with different target DNAs. The linear sweep voltammetry (LSV) curves showed an anodic peak current (i_{pa}) resulted from the oxidation of Hoechst 33258 and the current increased with the DNA hybridization amount increasing because Hoechst 33258 would bind to the minor groove of dsDNA (**Figure 5**). A weak i_{pa} of pDNA/PEI–hydrogel before hybridization might be resulted from the physical adsorption of Hoechst 33258 molecules on the surface of hydrogel or some existed fish sperm dsDNA.

The selective hybridization of target DNA with pDNA in the hydrogel electrode was further confirmed by fluorescence images. dsDNA strands can enhance the fluorescence of Hoechst 33258 considerably when it binds to the minor groove of dsDNA.[14] pDNA before hybridization or after incubation with non–complementary DNA showed very weak fluorescence and only some sporadically blue points were observed (Figure S9, Supporting Information). The blue area increases when the pDNA hybridizes with one–base mismatched DNA, which might be resulted from the formed part of dsDNA grooves. A largely blue fluorescence area is observed when the pDNA hybridizes with cDNA. The fluorescence signal of hydrogel

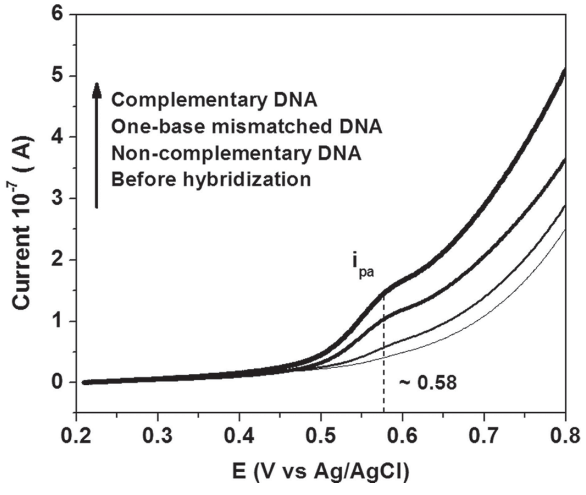

Figure 5. The LSV curves of hydrogel electrodes dyed with Hoechst 33258 before and after hybridization with different target DNAs. The concentrations of pDNA and target DNAs are 100 nM and 10^{-9} M, respectively.

before hybridization might be resulted from the physical adsorption of the dye molecules or the dye molecules binding to minor groove of fish sperm dsDNA. A little amount of fish sperm dsDNA might exist even though they were denatured at 95 °C to prepare hydrogel. However, the fluorescence images were focused on the surface of hydrogel. Therefore, the relative content of residual fish sperm dsDNA is lower and can be negligible. Of course, it needs more data to support the DNA hybridization on the surface of hydrogel.

We further used fluorescein (FAM)-labeled pDNA and Cy5-labeled target DNAs to investigate the hybridization (Figure S10, Supporting Information). The rugged hydrogel surface was prepensely selected for easy focus with high contrast because there is too strong fluorescence in smoothed surface (Figure S11, Supporting Information). Green fluorescence was observed for three hydrogels after FAM was excited, which means that pDNA had been adsorbed on the surface of hydrogel. Compared with one–base mismatched and non–complementary DNAs, cDNA after hybridization shows a strongly red fluorescence when Cy5 was excitated. The overlapped images show that pDNA and cDNA are in the same place. At the same time, the concentration of residual cDNA in solution after hybridization is lowest than that of other target DNAs (Figure S12, Supporting Information), which means that much more cDNA had been hybridized with pDNA in the hydrogel. The result further indicates that the DNA hybridization would happen on the surface of hydrogel and is consistent with the result of electrochemical experiments.

2.4. Detection of Real DNA Samples From Patients

The above result shows that the hydrogel electrode could detect the synthetic cDNA with high sensitivity and selectivity. Whether will it work well for the DNA from real samples? Mitochondrial DNA with high mutation rate and copy number in cancer cells is considered as an effectively molecular label for noninvasive diagnostics.[15] Therefore, mitochondrial DNA of ovarian cancer was selected to test the GO/DNA hydrogel electrode. Polymerase chain reactions were performed to amplify mitochondrial DNA. The products length is in the range of 456–512 bp (Preparation of mitochondrial DNA, Supporting Information). Mutations (16223C–T, 709G–A and 489T–C) were confirmed by DNA sequencing. **Figure 6** shows that the GO/DNA hydrogel electrode worked well and the linear range was from 1.0×10^{-9} to 1.0×10^{-12} M with the detection limit of 5.69×10^{-13}, 5.25×10^{-13} and 5.52×10^{-13} M for the three mutations, respectively, even though it was higher than that of synthetic cDNA. Three corresponding DNA samples without mutations from healthy adult were used to test the selectivity of GO/DNA hydrogel electrode. The result shows that normally mitochondrial DNA had low ΔR values even though in relatively higher concentrations. The effect of DNA length on the sensitivity of GO/DNA hydrogel electrode was also investigated. The result shows that shorter DNA had higher sensitivity (Figure S13, Supporting Information). This is ascribed to the high hybridization efficiency for short target DNA. Longer DNA has more intra–chain complementary region which could form hairpin structure, leading to less hybridization between the probe and target, which would result in weaker impedance change.

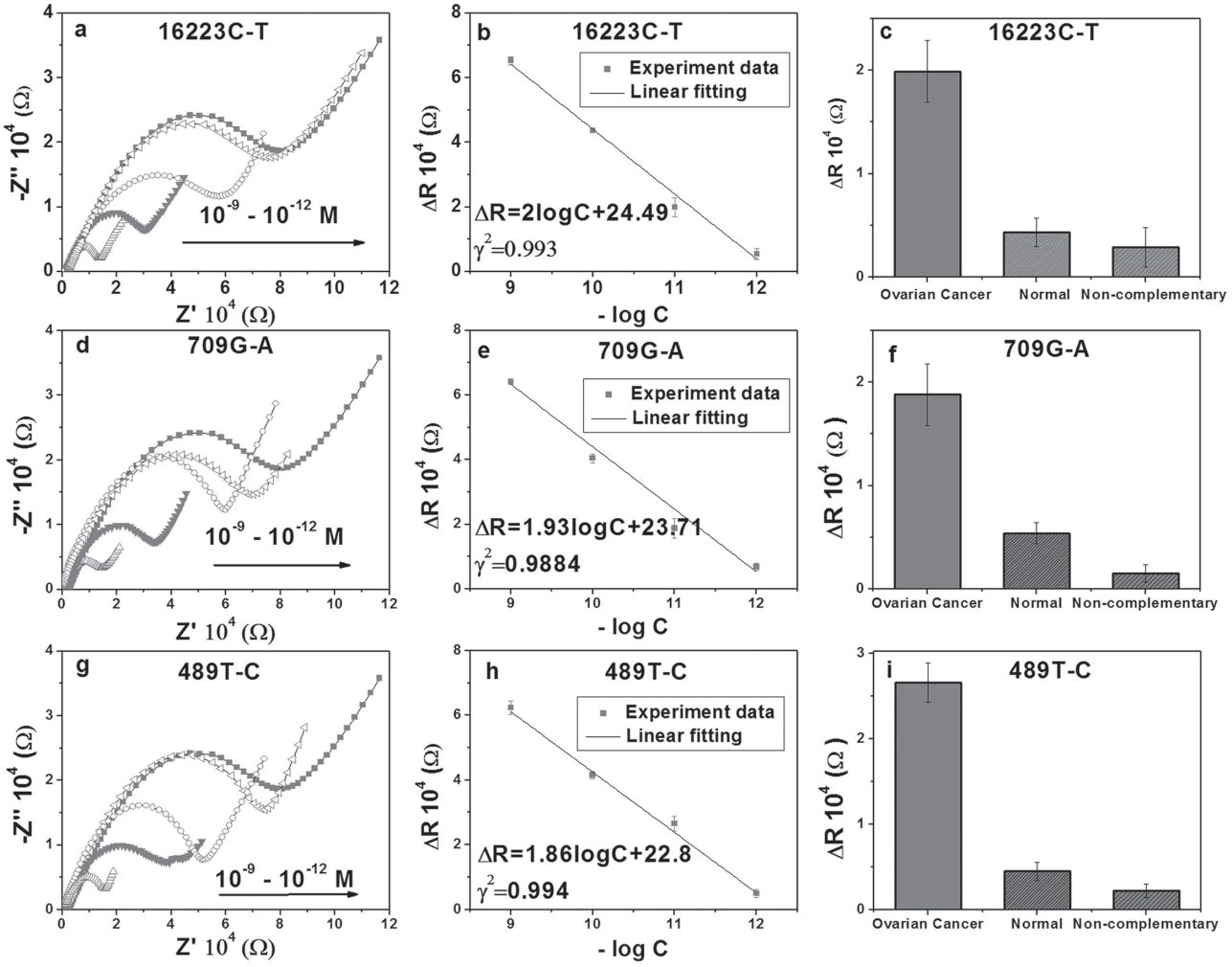

Figure 6. Detection of 16223C-T, 709G-A and 489T-C mutations in real DNA samples. PCR fragments were amplified from mitochondrial DNA of ovarian cancer patients. (a, d, g) Nyquist diagrams before and after hybridization with different concentrations of DNA. (b, e, h) Calibration plots of ΔR for detecting cDNA from ovarian cancer. (c, f and i) ΔR of pDNA/PEI–hydrogel electrode after hybridization with 1.0×10^{-11} M DNA of patient, 1.0×10^{-9} M DNA of normal adult and non-complementary DNAs. Data are the mean ± standard deviation of three different experiments.

2.5. Detection Mechanism

2.5.1. Effect of PEI

Based on above results, the hydrogel electrode demonstrates high sensitivity and selectivity. Therefore, more explanations on the performance of this sensor are necessary. PEI would play an important role in improving the sensitivity of DNA biosensor. The detection limit of the hydrogel electrode without PEI increased to 1.0×10^{-16} M (Figure S14, Supporting Information), which might be due to low adsorption of pDNA by electrostatic repulsion of negatively charged fish sperm DNA and GO in hydrogel. The zeta potentials of GO after addition of these components were used to support the adsorption and hybridization process (**Figure 7**). The zeta potential of GO was −31.6 mV. After addition of denatured fish sperm ssDNA, it increased to −37.8 mV due to the adsorption of negatively charged fish sperm ssDNA on the surface of GO. When PEI was added, the potential increased to 30.9 mV due to the

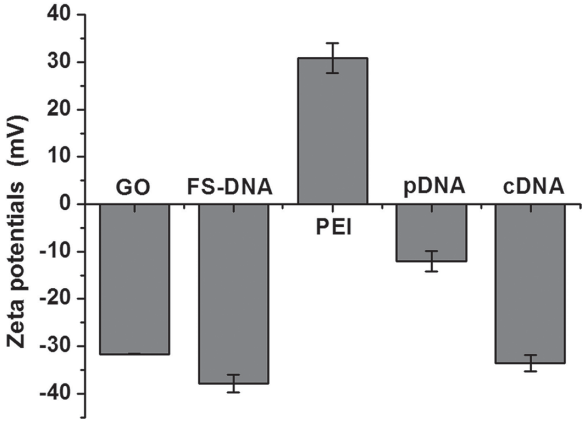

Figure 7. Zeta potential of the system after addition of each component. Data are the mean ± standard deviation of three different experiments. FS-DNA is fish sperm DNA.

adsorption of positively charged PEI. After immobilization of pDNA and hybridization with cDNA, the potential decreased to −12.0 and −33.5 mV, respectively. Therefore, the positively charged PEI could increase the immobilization amount of pDNA by electrostatic attraction, which benefits the improvement of sensitivity.

2.5.2. p–Type GO Doped by Negatively Charged DNA

The electronic structure alteration of GO caused by doping negatively charged DNA molecules would also improve the sensitivity of hydrogel electrode.[4] Similar results were reported that tethering of ssDNA onto GO led to a 128% increase in the conductivity, partially attributed to the attachment of the negatively charged DNA on the p–type GO; subsequent hybridization with cDNA increased the hole density, leading to a 71% increase in the conductivity.[16] The transport through GO is dominated by positive charge carriers (holes). As such, GO possesses a higher mobility than p-type polymer and just in the range suitable for room temperature electronics.[17] The result is similar to doped silicon that the conductivity of intrinsic silicon can be increased by adding certain impurities in minute quantities. Therefore, the conductivity of GO would be increased when minute DNA molecule was introduced, which would result in the conductivity of GO/DNA hydrogel increasing as shown in Figure 4a. In the meantime, the atomic thickness of GO would provide a strong bonding to DNA molecules. The short DNA fragments would act as charge carriers with higher mobility and could increase the hole density, leading to higher conductivity.[18] Our cDNA has 59 bases, and every base has a negative charge. Thus, every cDNA has 59 negative charges to dope GO. Therefore, the conductivity of GO/DNA hydrogel increased obviously. Therefore, the high sensitivity of this sensor could also be attributed to the conductivity change of p–type GO doped by negatively charged DNA.

2.5.3. Bionic Structure

The low detection limit of hydrogel electrode would be also ascribed to the bionic structure. The entrapment of fish sperm ssDNA and water in the hydrogel would result in a faster response or a faster diffusion of cDNA to pDNA. This hydrogel matrix provides an ideal environment for DNA and facilitates the hybridization of pDNA and cDNA.[19] The kinetics of adsorption and hybridization was studied by recording the relative impedance in different hybridization time (Figure S15, Supporting Information). The hybridization rate constant (1.2×10^{-2} s^{-1}) is higher than that ($1.0 \sim 9.8 \times 10^{-3}$ s^{-1}) of PEI–modified common electrodes,[20] which might be ascribed to the bionic interface of hydrogel containing rich water and fish sperm ssDNA molecules. Fitting the impedance data also yields the characteristic hybridization time of 30 min. The time is shorter than that of the classical methods with radioactive and optical labelling (hours to days).[21] Therefore, the bionic structure would benefit the hybridization of DNA and improve the sensitivity of the hydrogel electrodes. The bionic strucute means that the hydrogel contains natural molecules fish sperm ssDNA and high water amount, which is similar to the environment of DNA hybridization in biology. When the synthetic polymer polyvinyl alcohol (PVA) was used to replace fish sperm ssDNA (**Figure 8**a), the sensitivity of hydrogel was decreased. The result shows that it would be very important to improve the hybridization efficiency with naturally biological molecules as the component to prepare hydrogel. The high water content is very important to improve the sensitivity of hydrogel electrode (Figure S16, Supporting Information). Thus, it could be concluded that the hydrous circumstance would provide a nucleotide-friendly interface for probe immobilization and target hybridization.

2.5.4. Tunable Conductivity

The volume or thickness of hydrogel would affect the impedance of hydrogel (Figure 1 and 2). The hydrogel with a small volume would have a high conductivity. On the contrary, the hydrogel with a large volume would have a poor conductivity. The hydrogel with too high or too low conductivity is not sensitive to the weak conductivity change introduced by trace DNA. In order to further understand the effect of hydrogel thickness on impedance, we also used traditional method to coat the hydrogel on the surface of classical gold (Au) and glass carbon

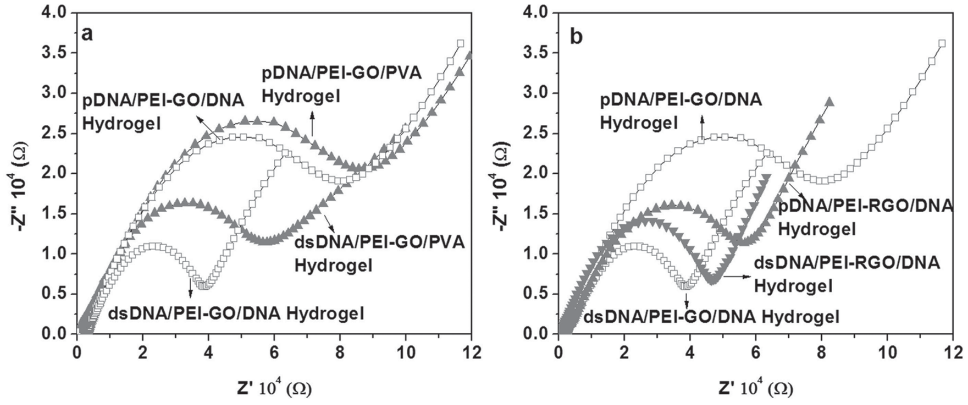

Figure 8. Effect of hydrogel component on DNA detection. a) Nyquist curves of GO/DNA hydrogel and GO/PVA hydrogel before and after hybridization with 1.0×10^{-15} M cDNA. b) Nyquist curves of GO/DNA hydrogel and RGO/DNA hydrogel before and after hybridization with 1.0×10^{-15} M cDNA.

(GC) electrodes with a small thickness. The detection limit increased to 1.0×10^{-17} M for both of Au and GC electrodes (Supplementary Figure S17). The high detection limit might be resulted from the high conductivity of hydrogel with a thin layer of hydrogel membrane.

The component of hydrogel would also affect the conductivity and sensitivity of hydrogel. GO and fish sperm DNA were displaced by RGO and PVA to prepare RGO/DNA and GO/PVA hydrogels, respectively. Figure 8 shows that the impedance changes after hybridization of these two hydrogels are smaller than that of GO/DNA hydrogel and the detection limit of 1.0×10^{-17} M for RGO/DNA hydrogel (Figure S18, Supporting Information) is higher than that of GO/DNA hydrogel, respectively. The result might be ascribed to the high conductivity of RGO and poor conductivity of PVA. Therefore, the conductivity of hydrogel would play an important role in improving the sensitivity of sensor, and it is very convenient to tune the conductivity of hydrogel by controlling the component and thickness of hydrogel.

3. Conclusions

Our work shows that the hydrogel electrode prepared from GO and fish sperm ssDNA with a bionic interface and tunable conductivity has an extremely low detection limit for DNA detection and a considerable application potential. The preparation of hydrogel electrode is simple and the cost is low. Therefore, the hydrogel electrode would be developed as a disposable product in clinic.

4. Experimental Section

Preparation of Hydrogel Electrode: GO was synthesized from graphite by the modified Hummers method as carried out in our previous work.[8] RGO was prepared in ammonia with hydrazine hydrate as reducing agent.[22] The preparation of GO/DNA hydrogel was based on the previous work of Shi et al.[5] Namely, 0.25 mL of GO (6 mg/mL) and 0.25 mL of fish sperm DNA sodium salt (10 mg/mL) were thoroughly mixed in a 2 mL of the cone bottom-centrifuge tube (clear microtubes MCT-200-C, Axygen), followed by heating at 95 °C for 5 min in a thermomixer to produce GO/DNA hydrogel. RGO/DNA hydrogel was prepared from 0.25 mL of RGO (2 mg/mL) and 0.25 mL of fish sperm DNA sodium salt (10 mg/mL) using similar to those presented above. 321 μL of GO dispersion (7.8 mg/mL) was added into 179 μL solution containing 1 mg PVA, then the mix was vibrated vigorously for 10 s, followed by a 20 min sonication to prepare GO/PVA hydrogel.[23] Then the lid of the tube was removed and the bottom was embedded with a copper wire of 4 centimeters (diameter is 1.0 mm) to produce hydrogel electrode (Scheme S1).

Impedance Measurements: Probe DNA (pDNA) and target DNA were dissolved in water to prepare a series of concentrations. 200 μL of PEI solution (1%) was added into the 2 mL of the cone bottom-centrifuge tube containing GO/PVA hydrogel. After 30 min, the PEI solution was pipetted out, and the hydrogel was rinsed with water for three times. 200 μL of pDNA solution (100 nM) was dropped into the tube and incubated for 30 min at 4 °C. Excess pDNA was removed by washing with water for three times. Alternating current impedance measurements were carried out in phosphate buffered saline (PBS) (pH 7.4) using an electrochemical workstation (CHI660C, CH Instrument). 3.0 M KCl–Ag/AgCl was the reference electrode and a platinum wire was the auxiliary electrode. Then the pDNA–immobilized hydrogel electrode was hybridized with different target DNAs. 200 μL of target DNA with designed concentration and 500 μL of PBS were added to the hydrogel electrode and incubated for 30 min at room temperature. The hydrogel was rinsed with water for three times to remove the excess target DNA. The impedance of hydrogel after hybridization was measured again in PBS (pH 7.4). The AC voltage amplitude was 5 mV and the voltage frequencies ranged from 0.1 Hz to 10^5 Hz. P1 and C1 sequences selected as the delegates of pDNA and target DNA (Table S3) are used in all measurements unless specially mentioned P2, P3, P4 and probes for 709G-A and 489T-C.

Supporting Information

Supporting Information is available from the Wiley Online Library or from the author.

Acknowledgements

This work is supported by the National Basic Research 973 Project (2014CB932004), National Natural Science Foundation of China (31371005, 81171453), the Knowledge Innovation Program of Shenzhen City (JCYJ20130327150937484), the Fundamental Research Funds for the Central Universities, Program for New Century Excellent Talents in University, the Ministry of Education.

Received: July 2, 2014
Published online: August 26, 2014

[1] a) F. Guerra, A. M. Perrone, I. Kurelac, D. Santini, C. Ceccarelli, M. Cricca, C. Zamagni, P. De Iaco, G. J. Gasparre, *Clin. Oncol.* **2012**, *30*, E373–E378; b) P. O. Van Trappen, T. Cullup, R. Troke, D. Swann, J. H. Shepherd, I. J. Jacobs, S. A. Gayther, C. A. Mein, *Gynecol. Oncol.* **2007**, *104*, 129–133.

[2] a) Y. Du, B. L. Li, E. K. Wang, *Acc. Chem. Res.* **2013**, *46*, 203–213; b) R. Miranda-Castro, N. de-los-Santos-Alvarez, M. J Lobo-Castanon, A. J. Miranda-Ordieres, P. Tunon-Blanco, *Electroanalysis* **2009**, *21*, 2077–2090.

[3] F. R. R. Teles, L. P. Fonseca, *Talanta.* **2008**, *77*, 606–623.

[4] W. S. Ji, W. H. Lee, J. H. Lee, H. Chou, R. D. Piner, Y. F. Hao, D. Akinwande, R. S. Ruoff, *Nano Lett.* **2013**, *13*, 1462–1467.

[5] Y. X. Xu, Q. Wu, Y. Q. Sun, H. Bai, G. Q. Shi, *ACS Nano.* **2010**, *4*, 7358–7362.

[6] a) E. Morles-Narvaez, A. Merkoci, *Adv. Mater.* **2012**, *24*, 313001; b) D. Reddy, L. F. Register, G. D. Carpenter, S. K. Banerjee, *J. Phys. D. Appl. Phys.* **2011**, *44*, 3499–3503; c) K. S. Novoselov, A. K. Geim, S. V. Morozov, D. Jiang, Y. Zhang, S. V. Dubonos, I. V. Grigorieva, A. A. Firsov, *Science* **2004**, *306*, 666–669.

[7] a) N. A. Peppas, J. Z. Hilt, A. Khademhosseini, *Adv. Mater.* **2006**, *18*, 1345–1360; b) D. S. Liu, E. J. Cheng, Z. Q. Yang, *NPG Asia Mater.* **2011**, *50*, 27–46; c) C. Li, G. Shi, *Adv. Mater.* **2014**, *26*, 3992.

[8] a) S. Naficy, J. M. Razal, G. M. Spinks, G. G. Wallace, P. G. Whitten, *Chem. Mater.* **2012**, *24*, 3425–3433; b) B. K. Adnadjevic, J. S. Colic, J. D. Jovanovic, *React. Funct. Polym.* **2013**, *73*, 1–19.

[9] a) J. Jia, L. P. Sun, N. Hu, G. M. Huang, J. Weng, *Small* **2012**, *8*, 2011–2015; b) J. Dong, J. B. Ding, J. Weng, L. Z. Dai, *Macromol. Rapid Comm.* **2013**, *34*, 659–664; c) J. Dong, J. Weng, L. Z. Dai, *Carbon* **2013**, *52*, 326–336; d) X. Lv, J. Weng, *Sci. Rep.* **2013**, *3*, 3285.

[10] a) M. B. Elizabeth, K. B. Jacqueline, *Struc. Biol.* **2002**, *12*, 320–329; b) M. B. Elizabeth, L. L. Alison, H. C. Nikolas, S. D. Sheila, K. B. Jacqueline, *Proc. Natl. Acad. Sci. USA* **2003**, *100*, 12543–12547.

[11] a) X. C. Dong, Y. M. Shi, W. Huang, P. Chen, L. J. Li, *Adv. Mater.* **2010**, *22*, 1649–1653; b) E. Dubuisson, Z. Y. Yang, K. P. Loh, *Anal. Chem.* **2011**, *83*, 2452–2460.

[12] a) M. N. Alam, M. H. Shamsi, H. B. Kraatz, *Analyst* **2012**, *137*, 4220–4225; b) T. Ito, K. Hosokawa, M. Maeda, *Biosens. Bioelectron.* **2007**, *22*, 1816–1819; c) B. Kannan, D. E. Williams, M. A. Booth, J. Travas-Sejdic, *Anal. Chem.* **2011**, *83*, 3415–3421; d) Y. Xu, H. Cai, P. G. He, Y. Z. Fang, *Electroanalysis* **2004**, *16*, 150–154.

[13] a) S. X. Wu, Q. Y. He, C. L. Tan, Y. D. Wang, H. Zhang, *Small* **2013**, *22*, 1027–1036; b) S. F. Wang, T. Z. Peng, C. F. Yang, *Electroanalysis* **2002**, *14*, 1648–1653.

[14] a) D. L. Boger, B. E. Fink, S. R. Brunette, W. C. Tse, M. P. Hedrick, *J. Am. Chem. Soc.* **2001**, *123*, 5878–5891; b) P. E. Pjur, K. Grzeskoviak, R. E. Dickerson, *Mol. Biol.* **1987**, *197*, 257–271.

[15] a) E. Palecek, M. Bartosik, *Chem. Rev.* **2012**, *112*, 3427–3481; b) L. Benesova, B. Belsanova, S. Suchanek, M. Kopeckova, P. Mnarikova, M. Lipska, M. Levy, V. Visokai, M. Zavoral, M. Minarik, *Anal. Biochem.* **2013**, *433*, 227–234.

[16] M. Nihar, B. Vikas, *Nano Lett.* **2008**, *8*, 4469–4476.

[17] a) X. Wu, M. Sprinkle, X. Li, F. Ming, C. Berger, W. A. de Heer, *Phys. Rev. Lett.* **2008**, *101*, 026801; b) T. V. Cuong, H. N. Tien, V. H. Luan, V. H. Pham, J. S. Chung, D. H. Yoo, S. H. Hahn, K. K. Koo, P. A. Kohl, S. H. Hur, E. J. Kim, *Phys. Status Solid A.* **2011**, *208*, 943–946; c) Y. Y. Lin, C. W. Chen, W. C. Yen, W. F. Su, C. H. Ku, J. J. Wu, *Appl. Phys. Lett.* **2008**, *92*, 233301.

[18] H. Ma, R. W. R. Wallbank, R. Chaji, J. Li, Y. Suzuki, C. Jiggins, A. Nathan, *Sci. Rep.* **2013**, *3*, 2730.

[19] a) J. Kopecek, *Biomaterials* **2007**, *28*, 5185–5192; b) S. K. Seidlits, R. M. Gower, J. A. Shepard, L. D. Shea, *Expert Opin. Drug. Del.* **2013**, *10*, 499–509; c) L. Cavicchioli, *Biofutur* **2013**, *340*, 14–14.

[20] a) J. Weng, J. F. Zhang, H. Li, L. P. Sun, C. H. Lin, Q. Q. Zhang, *Anal. Chem.* **2008**, *80*, 7075–7083; b) G. L. Luque, N. F. Ferreyra, A. Granero, S. Bollo, G. A. Rivas, *Electrochim. Acta.* **2011**, *56*, 9121–9126.

[21] a) X. Su, X. J. Xiao, C. Zhang, M. P. Zhao, *Appl. Spectrosc.* **2012**, *66*, 1249–1261; b) K. M. Wang, J. Huang, X. H. Yang, X. X. He, J. B. Liu, *Analyst.* **2013**, *138*, 62–71.

[22] D. Li, *Nat. Nanotechnol.* **2008**, *3*, 101–105.

[23] H. Bai, C. Li, X. L. Wang, G. Q. Shi, *Chem. Comm.* **2010**, *46*, 2376–2378.